Low-power Radio Galaxies in the Distant Universe: A search for FR I at $1 < z < 2$ in the COSMOS field

Marco Chiaberge[1,2], Grant Tremblay[1,5], Alessandro Capetti[3], F. Duccio Macchetto[1], Paolo Tozzi[4], W. B. Sparks[1]

chiab@stsci.edu

Received _____; accepted _____

Accepted for publication in ApJ

[1]Space Telescope Science Institute, 3700 San Martin Drive, Baltimore, MD 21218

[2]INAF - IRA, Via P. Gobetti 101, I-40129 Bologna, Italy

[3]INAF - Osservatorio Astronomico di Torino, Via Osservatorio 20, I-10025 Pino Torinese, Italy

[4]INAF - Osservatorio Astronomico di Trieste, Via Tiepolo 11, I-34143 Trieste, Italy

[5]Rochester Institute of Technology, One Lomb Memorial Drive, Rochester, NY 14623 USA

ABSTRACT

We present a search for FR I radio galaxies between $1 < z < 2$ in the COSMOS field. In absence of spectroscopic redshift measurements, the selection method is based on multiple steps which make use of both radio and optical constraints. The basic assumptions are that 1) the break in radio power between low-power FR Is and the more powerful FR IIs does not change with redshift, and 2) that the photometric properties of the host galaxies of low power radio galaxies in the distant universe are similar to those of FR IIs in the same redshift bin, as is the case for nearby radio galaxies. We describe the results of our search, which yields 37 low-power radio galaxy candidates that are possibly FR Is. We show that a large fraction of these low-luminosity radio galaxies display a compact radio morphology, that does not correspond to the FR I morphological classification. Furthermore, our objects are apparently associated with galaxies that show clear signs of interactions, at odds with the typical behavior observed in low-z FR I hosts. The compact radio morphology might imply that we are observing intrinsically small and possibly young objects, that will eventually evolve into the giant FR Is we observe in the local universe. One of the objects appears as point-like in HST images. This might belong to a population of FR I-QSOs, which however would represent a tiny minority of the overall population of high-z FR Is. As for the local FR Is, a large fraction of our objects are likely to be associated with groups or clusters, making them "beacons" for high redshift clusters of galaxies. Our search for candidate high-z FR Is we present in this paper constitutes a pilot study for objects to be observed with future high-resolution and high-sensitivity instruments such as the EVLA and ALMA in the radio band, HST/WFC3 in the optical and IR, JWST in the IR, as well as future generation X-ray satellites.

Subject headings: galaxies: active — galaxies: elliptical and lenticular, cD — galaxies: high-redshift

1. Introduction

Among the most energetic phenomena in the universe, radio galaxies are excellent laboratories in which we investigate some of the major challenges of today's astrophysics, such as accretion onto supermassive black holes (SMBH), the associated formation of relativistic jets (e.g. Blandford et al. 1990; Livio 1999), the feedback processes of an "active" SMBH in the star formation history of a galaxy (e.g. Hopkins et al. 2006) and the role of the AGN in injecting energy in the intracluster medium (Fabian et al. 2006). The original classification of radio galaxies is based on their radio morphology: "edge-darkened" (FR I), are those in which the surface brightness decreases from the core to the edges of the source, and typically display large lobes or plumes; "edge-brightened" (FR II), are those in which the peaks of the brightness is located near the edges of the radio source. FR I galaxies typically have a radio power lower than that of FR II sources, with the FR I/FR II break set at $L_{178\mathrm{MHz}} \sim 2 \times 10^{33}$ erg s^{-1} Hz^{-1} (Fanaroff & Riley 1974). However, the transition is rather smooth and both radio morphologies are present in the population of sources around the break. The FR I/FR II break (at low redshifts) also depends on the luminosity of the host galaxy, as shown by Owen & Ledlow (1994); Ledlow & Owen (1996). However, it is still unclear whether or not that might simply be a result of selection effects (Scarpa & Urry 2001). From the optical point of view, FR Is are invariably associated with the most massive galaxies in the local universe (e.g. Zirbel 1996; Donzelli et al. 2007), thus they are also most likely to be linked with the most massive black holes in the local universe. Furthermore, FR Is are usually located at the center of massive clusters (see e.g. Owen 1996, for a review). On the other hand, at low redshifts, FR IIs are generally found in regions of lower density, while some FR II reside in richer groups or clusters at redshifts higher than ~ 0.5 (Zirbel 1997).

Finding high-z FR Is and understanding their evolution will help us to address a

number of other unsolved problems in current astrophysics, such as studying the properties of the "building blocks" of massive elliptical galaxies present in today's universe, assessing the relationship between giant elliptical and their central supermassive black holes, and studying the formation and evolution of galaxy clusters.

However, flux-limited samples of radio galaxies such as the 3CR and its deeper successors 6C and 7C catalogs are limited by the tight redshift-luminosity correlation, i.e. the well known Malmquist bias. This, along with the steep luminosity function of these objects, gives rise to a selection bias resulting in detection of high luminosity sources only at high redshifts and low power sources exclusively at low redshift. It is therefore unsurprising that, in the above mentioned catalogs, all "high z" objects are FR II sources (or QSOs), while FR Is are only found at $z < 0.2$. Indeed, besides possibly one of the two candidates discussed in Snellen & Best (2001), no FR I radio galaxies are known at $z > 1$. Nevertheless, there is evidence that the population of radio-loud AGN substantially increases with redshift up to $z \sim 2 - 2.5$ (e.g. Ueda et al. 2003). Thus, if FR I galaxies do in fact exist at high redshift, they might be significantly more abundant at $z > 1$ than in the local universe. Interestingly, Sadler et al. (2007) find that in the redshift range $0 < z < 0.7$ radio galaxies with radio powers $P_{1.4} < 10^{25}$ W Hz^{-1} undergo significant evolution. Their result is consistent with being pure luminosity evolution, which follows a law similar to that followed by star forming galaxies over a similar redshift range. Clearly, finding radio galaxies of low power at higher redshift is extremely important to achieve a broader understanding of the cosmological evolution of these sources, as compared to the evolution of normal galaxies.

The role of FR Is in the framework of the unification scheme for radio-loud AGN is a significant matter of debate. In particular, the lack of low redshift "FR I quasars" (defined as radio galaxies with FR I morphology associated with objects showing broad emission

lines in their optical-UV spectrum), with the possible exception of a few peculiar objects, such as the broad-lined FR I 3C 120 (e.g. Eracleous & Halpern 1994; García-Lorenzo et al. 2005), is still to be understood. It is possible that most, if not all, FR Is intrinsically lack a broad line region and are possibly powered by low radiatively efficient accretion disks (e.g. Baum et al. 1995; Falcke et al. 2004; Fabian et al. 2006). This picture is also supported by the discovery that the large majority of FR I hosts have faint unresolved nuclei in HST images, whose flux and luminosity show a tight correlation with that of the radio cores (Chiaberge et al. 1999). The existence of such a correlation is explained in terms of a single emission mechanism (non-thermal synchrotron radiation produced at the base of the relativistic jet) for both the radio and the optical band (Chiaberge et al. 1999). On the other hand, recent work (Heywood et al. 2007) claims that FR I quasars are prevalent in the universe, based on the analysis of a sample of QSOs in the redshift range $0.36 < z < 2.5$ selected from the 7C survey, using both their low-frequency flux density and optical spectral properties. However, some of their results are still unclear. For example, these authors show evidence for the existence of "high-power" FR I QSO, whose nature has yet to be completely understood. A search for "bona fide" low power radio galaxies at $1 < z < 2$ can clearly help to achieve a better understanding of the FR I-QSO phenomenon and its role in the framework of the AGN unification models.

From the point of view of the environment, FR I radiogalaxies are found in giant ellipticals often located at the center of clusters of galaxies. Finding high-z FR I with properties similar to those found in the local universe can be a breakthrough for studies of the evolution of galaxies and clusters. Using radio galaxies as beacons of high-z clusters is not a new idea. In the recent past, high-z radio galaxies have often been used to find protoclusters and massive galaxies at the epoch of their formation (e.g. Pentericci et al. 2001; Zirm et al. 2005; Miley & De Breuck 2008). However, all the above studies used high power sources with extremely high redshifts ($z > 2$). These are rare objects in the universe

whose connection to today's radio galaxies is not clear. It is also unclear whether their protocluster environment have virialized by that epoch, since it is difficult to detect the X-ray emission of the ICM. Powerful FR IIs have the disadvantage of having strong emission from the nucleus and powerful relativistic plasma jets, which may strongly influence the properties of the host galaxy and may hamper studies of the environment, in particular in the X-ray band (e.g Fabian et al. 2003). FR Is are less powerful AGNs, they are more similar to "normal" inactive galaxies than FR IIs, and allow us an easier investigation of the surrounding environment, with dramatic impact on cosmological studies. FR Is with distorted morphologies were used to search for clusters, but only out to a redshift $z < 1$ (Blanton et al. 2000). To date, only a handful (less than 10) X-ray confirmed clusters are known at $z > 1$, and none of them is at a redshift higher than 1.45 (see Rosati et al. 2002, for a review). The clusters associated with our FR I candidates might in fact be the "missing link" between the protoclusters at redshifts > 2 and the well studied clusters of galaxies at $z < 1$.

In order to perform our search for FR Is in the unexplored range of redshift between z=1 and 2, we take advantage of the large collection of multi-wavelength data collected by the COSMOS collaboration (Scoville et al. 2007). In section 2 we give an overview of our method, while in section 3 we describe our selection procedure in details. In section 4 we give details about a few peculiar objects for which the optical counterpart identification is uncertain, but the host galaxy is clearly seen in the IR, and in section 5 we discuss our results from the point of view of their radio morphology, local environment and we show a few cluster candidates. In section 6 we give a summary of the work, draw conclusions and outline some future perspectives.

Throughout this paper we use WMAP cosmology (H_0=71, Ω_M =0.27, Ω_{vac} = 0.73). For the magnitudes of the sources we adopt the Vega system.

2. Overview of our search for high-z FR Is

The search for FR I radio galaxy candidates between $1 < z < 2$ is performed using selection criteria in multiple wavelengths. As already pointed out in the previous section, flux limited samples of radio galaxies include low power sources at low redshift only. The 3C sample, which is arguably the best studied sample of radio galaxies, with his flux limit set at 10 Jy at 178MHz, includes FR I radio galaxies only up to $z \sim 0.2$. Deeper catalogs may include a larger number of distant FR Is, however, a search for FR Is based on the radio flux only, is extremely inefficient, because of the dominant population of faint radio sources associated to e.g. nearby starburst galaxies. In other words, by using deep flux limited samples we would find a multitude of sources whose radio flux is typical of that of an FR I at $z \sim 1$, for example, but are in fact low-z starburst galaxies (or, alternatively, they might even be high power FR IIs at $z > 2$), and very few *bone fide* FR Is. In order to select the right objects, it is therefore crucial that our search discriminate each candidate not only by radio power, but also by its properties across multiple bands.

We focus our search within the overlapping fields of the Very Large Array Faint Images of the Radio Sky at Twenty-centimeters (VLA FIRST) survey (Becker et al. 1995) and the cross-spectrum Cosmic Evolution Survey (COSMOS, Scoville et al. 2007). The COSMOS field, a $1.4^\circ \times 1.4^\circ$ square centered at R.A.=10:00:28.6, DEC=+02:12:21.0 (J2000) is entirely covered by FIRST. The COSMOS region was selected because its equatorial position allows for observations from northern and southern-hemisphere observatories, as well as for its low and uniform galactic extinction $\left(\langle E_{(B-V)} \rangle \simeq 0.02 \text{ mag}\right)$ and lack of very bright radio, UV, and X-ray sources. This 2 square degree region of the sky has been extensively imaged across the spectrum with deep observations from most of the major space- and ground-based observatories, yielding a rich dataset of over 2 million galaxies in multiple bands. The specific COSMOS datasets used in our selection procedure consist of 1.4 GHz

radio imaging from the VLA (Schinnerer et al. 2007), as well as optical images taken with *HST*'s Advanced Camera for Surveys (ACS/WFC, Koekemoer et al. 2007) and the F814W filter (similar to i-band), in K_s-band from the Kitt Peak National Observatory (KPNO, Capak et al. 2007), in optical bands from Subaru (Taniguchi et al. 2007), and in i and u-band from the Canada-France-Hawaii Telescope (CFHT, Capak et al. 2007). We also make use of less sensitive imaging across multiple optical bands from the *Sloan Digital Sky Survey* (SDSS, York et al. 2000) Data Release 5 (DR5).

Our search procedure begins with the FIRST survey at 1.4 GHz. The low resolution FIRST data allow us to easily start our selection procedure based on the "total" radio flux. FIRST was initially conceived as a radio sky counterpart to the Palomar Observatory Sky Survey (POSS I), and so encompasses over 10,000 square degrees of the North Galactic Cap (which includes the full COSMOS field), imaged in 3 minute snapshots with 2×7 3-MHz frequency channels centered at 1.365 and 1.435 GHz in the VLA's B-configuration (Becker et al. 1995). Post-pipeline radio maps have a resolution of $5''$, and the detection threshold of the survey is of order ~ 1 mJy with a typical RMS of 0.15 mJy. At redshift $z = 1.5$ $5''$ corresponds to 40 kpc. Since FR I radio galaxies exhibit jet structures at a few times 100 kpc scales, very little morphological information is discernible from the 1.4 GHz FIRST images. However, higher resolution maps would have the disadvantage of missing some of the extended, lower surface brightness regions, therefore the FIRST survey is the right catalog to begin our search with.

At the 1 mJy detection threshold of the survey, ~ 90 sources per square degree are detected. The low angular resolution of FIRST is compensated for by the VLA-COSMOS survey (Schinnerer et al. 2007), which has a resolution of $1''.5 \times 1''.4$ which corresponds to ~ 12 kpc for a source at $z = 1.5$, and a detection threshold of 10 μJy (1-sigma). We therefore use the FIRST images only to obtain the total radio flux of the sources. We use

the deeper and higher resolution VLA-COSMOS data to study the actual radio structure of the sources that meet our initial flux selection and derive their position, as detailed in the next section.

Note that sources are not selected based on their "FR I" radio morphology, but just using the fact that FR I radio galaxies are low power radio sources. However, we do use the radio morphology to exclude FR IIs. Therefore, at the end of our selection process, we are left with a sample of low power radio sources that are FR I candidates, and whose radio morphology still has to be determined in greater detail.

3. Selection Procedure

Our search depends upon the assumption that the FR I/FR II break luminosity at $L_{1.4\ \mathrm{GHz}} \sim 4 \times 10^{32}$ erg s^{-1} Hz^{-1} (assuming a spectral index $\alpha_r = 0.8$ between 1.4 GHz and 178 MHz) does not change with redshift. Moreover, we assume that the photometric properties of high-z FR I host galaxies are similar to those of FR II hosts in the same range of redshift. Note that photometric redshifts for COSMOS sources are already available in the literature Mobasher et al. (2007). Photometric redshifts have proved to be statistically

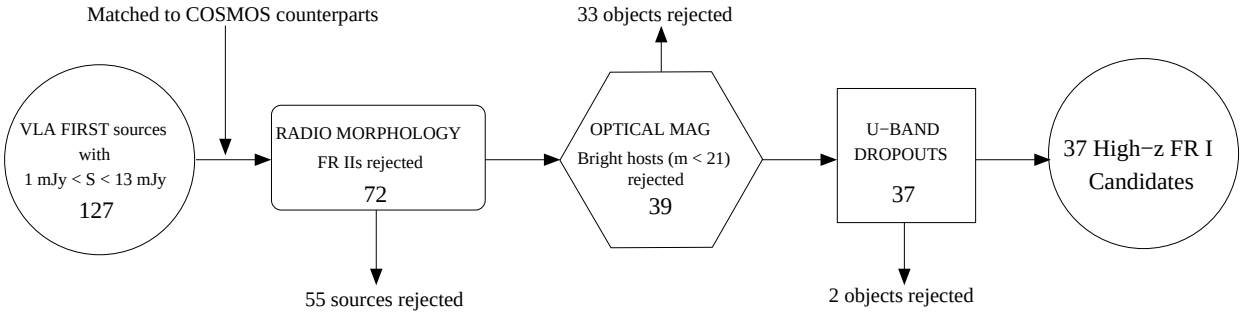

Fig. 1.— Flow-chart describing our selection procedure. The number of sources that survive each rejection step is reported inside each box. See text for more details.

reliable for a large population of objects, but for single objects (and for AGN in particular) the uncertainty of z_{phot} can be large. Therefore, we use photometric redshifts only as a confidence check (see Sect.5), and not to confirm or discriminate among candidates. That is, no objects meeting our selection criteria are rejected based on photometric redshift value. Based on these two basic assumptions outlined above, we describe our selection procedure in the following. A flow-chart describing our selection procedure is shown in Fig 1.

1. **Radio selection: flux limits.** We select FIRST radio sources inside the COSMOS field whose 1.4 GHz total flux corresponds to that expected for FR Is at $1 < z < 2$. To that end, we require that our candidate sources reside in a narrow bin of $L_{1.4}$. The limits of this "allowable" 1.4 GHz luminosity range ($L_{1.4,\rm min}$, $L_{1.4,\rm max}$) are set such that the objects we select have a total radio power typical of FR Is. That is, the radio power must be significantly *above* the level of radio activity produced by "non radio-loud AGN" and starburst galaxies[1] in the target redshift bin, but safely *below* the FR I/FR II break. Based on these criteria, we calculate $L_{1.4,\rm min}$ and $L_{1.4,\rm max}$ in terms of flux limits $F_{1.4,\rm min}$ and $F_{1.4,\rm max}$. We set $F_{1.4,\rm min}$ to correspond to the flux observed from a source of radio power $L_{1.4,\rm min}$ at $z = 2$ (e.g. the faintest of the objects we're searching for), and set $F_{1.4,\rm max}$ to the flux of a source of brightness $L_{1.4,\rm max}$ at $z = 1$ (e.g. the very brightest sources we wish to find). The observed flux of the $\nu = 1.4$ GHz Fanaroff-Riley break luminosity for each value of z can be derived using

$$F_\nu\left(\nu_0\right) = \frac{L_\nu\left(\nu_0\right)\left(1+z\right)^{1-\alpha}}{4\pi D_L^2}, \tag{1}$$

where $L_\nu(\nu_0)$ is the luminosity of the FR I/FR II break at ν_0. We assume a spectral index $\alpha = 0.8$. In the formula, a factor of $(1+z)$ accounts for the passband and another of $(1+z)^{-\alpha}$ makes up the K correction. The flux of the FR I/FR II break at $z = 1$ is $F_{1.4} \sim 26$ mJy. However, we set our upper "allowable flux" limit $F_{\rm max}$ a factor of two

[1]Starburst galaxies typically have $L_{1.4} < 10^{30}$ erg s^{-1} Hz^{-1}.

fainter than this (to 13 mJy) to ensure that, at the end of the process, we select "bona fide" FR I candidates and avoid accidentally selecting FR IIs near the break luminosity. However, these FR IIs are rejected during step 2. based on their radio morphology. The flux of the break at $z = 2$ is ~ 10 mJy, and so we set our lower limit $F_{\rm min}$ to be an order of magnitude fainter (at 1 mJy). This corresponds to the detection threshold of the FIRST survey. We searched the FIRST database (`http://sundog.stsci.edu/`) for radio sources possessing integrated 1.4 GHz fluxes between 1 mJy and 13 mJy within the COSMOS field. The number of sources that match our flux criteria is 131. Clearly, a selection based on flux only allows the presence of both $z < 1$ "faint" sources and $z > 2$ "powerful" sources. The next selection steps are designed to reject most of the objects that fall outside our preferred redshift range.

2. **Radio selection: morphology.** The sources selected at step 1 are individually examined for large-scale radio morphology. Those candidates featuring clearly "edge-brightened" radio structures are rejected, so as to filter out more powerful FR II sources at redshift $z > 2$ which have passed our initial flux selection. Though the FIRST imaging is at very low resolution, it typically suffices for the identification of classical doubles, as edge-brightened lobes or hotspots of FR IIs are found on >100 kpc scales, which translates into $> 11''$ at $z = 2$. As a result of this, a significant number of pairs of radio sources that were counted as two "single" objects at the previous step are now recognized to be "double" sources. Twenty-two of those FR IIs are identified. In Fig. 2 we show three examples of such sources. Note that these account for 44 "single" FIRST radio sources. We then check the VLA-COSMOS radio maps to make sure that objects that appear as compact in the FIRST images are not smaller "double" FR II radio sources. Eleven FR IIs are identified using VLA-COSMOS radio maps, for a total of 55 such objects rejected based on their radio morphology.

3. **Optical selection: magnitude.** In order to set constraints on the host galaxies' photometric properties, the next step involves the identification of the optical counterparts of the radio sources. Therefore, for our sample, the optical counterpart identification is part of our selection process. The method we use is simply to blink the COSMOS-VLA radio data with the optical COSMOS-HST image, registered on the same WCS framework. Despite the short exposure time (single orbit observations), the COSMOS-HST images are the most suitable data for identifying the optical counterparts. The significantly higher angular resolution, as compared to the ground based optical data, allows us to avoid confusion. In most cases, it is straightforward to identify the host galaxy, since the position of the radio core is well set by the COSMOS-VLA images, and the beam size is small enough that only one galaxy is found at the same position on the HST image. We will discuss a few peculiar cases for which the optical counterparts are not easily detected in section 4. We also unambiguously identify the host galaxy for 24 FR IIs. We check the COSMOS source catalog at the coordinates corresponding to the radio sources that match the first two selection steps and we obtain the magnitudes of each object in different bands.

We set a lower limit in optical (i-band) magnitude to reject fairly bright low redshift galaxies with intrinsically less powerful radio emission (e.g. possibly star forming galaxies). In this step we make use of the assumption that the properties of the host galaxies of FR Is are similar to those of FR IIs, as it is the case for low-redshift radio galaxies. The K-band magnitude of an FR II radio galaxy at $1 < z < 2$ is known not to exceed $M_K \sim 17$ (e.g. Willott et al. 2003), and the typical I-K color of FR II hosts is ~ 4 or higher. This sets a lower limit to the i-band magnitude of ~ 21. In Fig. 3 we plot the i-band magnitude against the radio flux for the sources with an optical counterpart. Note that not all of the FR IIs are plotted in the diagram: some of the FRIIs are left out because either the host galaxy is not detected in the optical, or it cannot be identified because it lies somewhere between the location of the two radio hotspots and multiple galaxies are present in the same region. For

the candidate FRIs that do not have an optical counterpart but for which the host galaxy is seen in the IR only (see Sect 4), we plot the magnitude of the closest optical source. This can be interpreted just as a lower limit to magnitude of the host and it is completely irrelevant from the point of view of the sample selection, since we do not discard optically faint objects.

Note that, as a result of the magnitude limit, most of the host galaxies of our candidates are not detected in the Sloan Digital Sky Survey. This step in the selection process is only intended to reject those host galaxies that are unreasonably brighter or bluer than typical radio galaxies in the target redshift range. Importantly, setting a limit in i-band ensures us that we are not rejecting galaxies that are fainter than "normal" radio galaxies in K-band. With this selection step we only filter out bright nearby galaxies, and we are keeping in our sample distant and intrinsically red objects. Thirty-three objects are rejected at this stage because of the host galaxy optical brightness.

One object with $m_I < 21$ (object 236) is not rejected because it appears to be "stellar-like" in the HST image. Since it completely lacks the host galaxy, the magnitude of the point source we observe can be considered as a lower limit to the magnitude of the host. The nature of this source is unclear: one possibility is that it is a QSO that resides in the redshift range $1 < z < 2$. In that case, because of its low radio power, it would represent an interesting case of FR I-QSO (see Section 5). Alternatively, it could be a high-power radio-loud QSO located at a redshift higher than 2.

4. **Optical selection: u-band dropouts.** As the last step in the selection process, we want to make sure to include in our sample objects with redshift not significantly higher than 2. This is mainly because the radio power of those objects would exceed the FR I/FR II break. We check the deep COSMOS ground based images and we reject two sources that are detected in V and B-band, but not in the U-band. Such "u-band dropouts"

are typically galaxies located at a redshift significantly higher than our range of interest, with a lower limit at $z \sim 2.5$ (e.g. Giavalisco 2002).

At the end of the selection process we are left with 37 candidates, that are listed in Table 1. The Table reports, for each source, the radio flux at 1.4 GHz, the magnitude of the optical counterpart in K_s, V and i band (in the Vega system), the photometric redshift of the source as it appears in the COSMOS catalog (Mobasher et al. 2007), and a qualitative description of the observed radio and optical morphologies.

Radio and optical images for each of the FR I candidates are shown in Figs. 4, 5 and 6. The radio data at 1.4 GHz are taken from the VLA-COSMOS survey (Schinnerer et al. 2007). The optical images are from the HST-COSMOS programs (GO 9822, GO 10092) and were taken using *HST*/ACS in *i*-band (Koekemoer et al. 2007), unless mentioned otherwise.

In the following section we discuss issues related to the optical counterpart identifications. Note that the identification of the optical counterparts is part of our selection process at steps 3 and 4. In fact, we look both at the shallow SDSS images (mainly to check that no optical counterpart is found, as prescribed by our selection step 2) and at the deeper ground based images from the COSMOS collaboration (to identify the optical counterpart). In the next section we describe a few peculiar cases of objects that show no optical counterpart but are clearly detected in th IR.

4. IR identifications

In a few cases the optical identifications are difficult. This generally happens because either no obvious optical source co-spatial with the radio core is seen, or it is not clear whether we are seeing a group of galaxies or a single irregularly shaped object. In six cases,

the peak of the optical emission is not coincident with the peak of the radio core. This is clearly shown in the case of our candidates 5, 7, 22, 32, 39 and 228 (see Figs. 5). For object 5, a very low surface brightness object is only tentatively detected in the ACS image, even after significant smoothing. For object 22, the optical counterpart is also not clearly identified, since 3 to 4 relatively bright galaxies are present in the ACS image, but none of them appears to be co-spatial with the peak of the radio core. For objects 7, 39 and 228 no optical counterpart is detected anywhere near the location of the radio source. For object 32 an optical source is clearly seen in the Subaru i-band image, but it is located $\sim 2''$ E of the radio source. However, in all cases, *Spitzer Space Telescope*/IRAC images taken as part of the COSMOS program (Sanders et al. 2007) clearly reveal the host galaxy at the location of the radio source. In Fig. 7 we show the *Spitzer* images at 3.6 μm, together with the radio contours that indicate the location of the FR I candidate. Clearly, the optical magnitude listed in Table 1 for the objects that are only identified in the IR should be consider as a lower limit, since it has been derived from the COSMOS catalog from the optical object closest to the radio source.

The lack of an optical counterpart, together with the detection of the IR counterpart is intriguing. The absence of the object in the ACS image might be explained by the fact that the host galaxy is a very low surface brightness object, thus the short exposure time of the HST images, together with the small collecting area of the telescope does not allow us to detect it. However, we would expect to detect it in the deeper ground based images. This cannot be clearly established, mostly because of confusion problems. In the IR Spitzer images, the elliptical host can be more easily seen, since it dominates the emission with respect to the bluer surrounding galaxies that disappear in the IR. An alternate scenario is that these are higher redshift objects, not visible in the optical because of Hydrogen absorption (i-band dropouts). In this case, the bluer galaxies seen in the optical data around the position corresponding to the radio source would not be at the same redshift as

the host galaxy of the radio source. For an i-band dropout, the redshift of the host would be around $z \sim 6$, therefore these objects would be high power radio sources that should not be included in our sample. Further investigation is needed to assess their nature. It is also worth noting that for these objects with uncertain optical identification, z_{phot} is most likely derived from one of the galaxies surrounding the real host.

Table 1. $1 < z < 2$ FR I Radio Galaxy Candidates

ID	K_s Mag	V Mag	I Mag	$S_{20\ \mathrm{cm}}$ (mJy)	z_{phot}	Radio Morphology	Optical Morphology
(1)	(2)	(3)	(4)	(5)	(6)	(7)	(8)
01	17.710	24.423	21.860	1.79	0.94	Compact	Smooth
02	19.279	25.835	24.047	1.08	1.59	Extended	Compact
03	21.014	25.583	25.008	4.21	1.59	Unresolved	Compact
04	18.872	25.473	23.957	5.99	1.85	Extended	Compact
05	18.991	24.449	23.789	1.30	2.08	Compact	–
07	20.072	24.942	23.777	1.14	1.09	Compact	–
11	19.716	26.994	24.750	1.13	1.05	Compact	Compact
13	18.670	24.711	22.835	1.51	1.21	Compact	Compact
16	18.668	24.860	22.741	5.70	1.10	Unresolved	Smooth
18	19.015	24.316	22.479	4.39	0.93	Extended	Complex
20	18.276	24.594	21.998	1.33	0.98	Extended	Compact
22	19.698	24.043	23.288	2.74	1.51	Compact	–
25	18.787	24.952	23.266	2.18	1.40	Compact	Complex
26	17.631	24.908	22.332	1.88	1.30	Extended	Smooth
27	18.722	24.279	22.957	1.91	1.39	Compact	Complex
28	20.158	25.127	24.118	1.77	1.23	Compact	Compact
29	21.099	25.341	24.610	2.12	1.03	Compact	Compact
30	18.360	25.812	23.055	1.26	1.15	Compact	Complex
31	18.456	23.948	21.981	3.71	0.88	Compact	Smooth
32	20.214	25.095	24.134	1.31	2.17	Compact	Compact

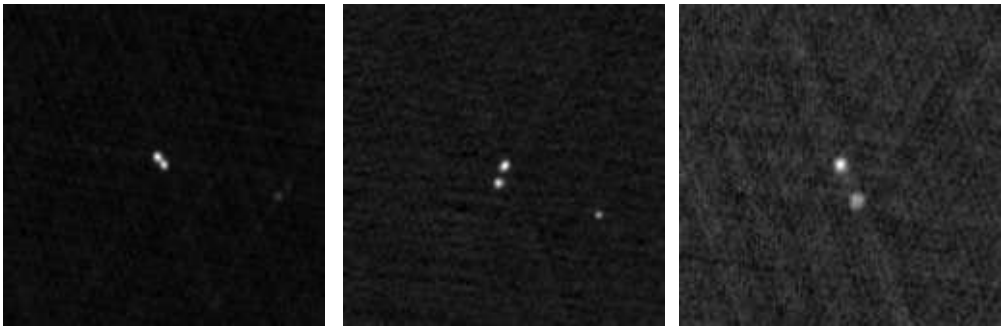

Fig. 2.— Examples of sources showing a clear double (FR II) morphology that were rejected during our selection step 2. The objects are the FIRST sources J095908+024809 (left), J100217+012220 (center) J100245+024534 (right). The size of each image is 5'x5', as obtained from the FIRST image cutouts archive at `http://third.ucllnl.org/cgi-bin/firstcutout`.

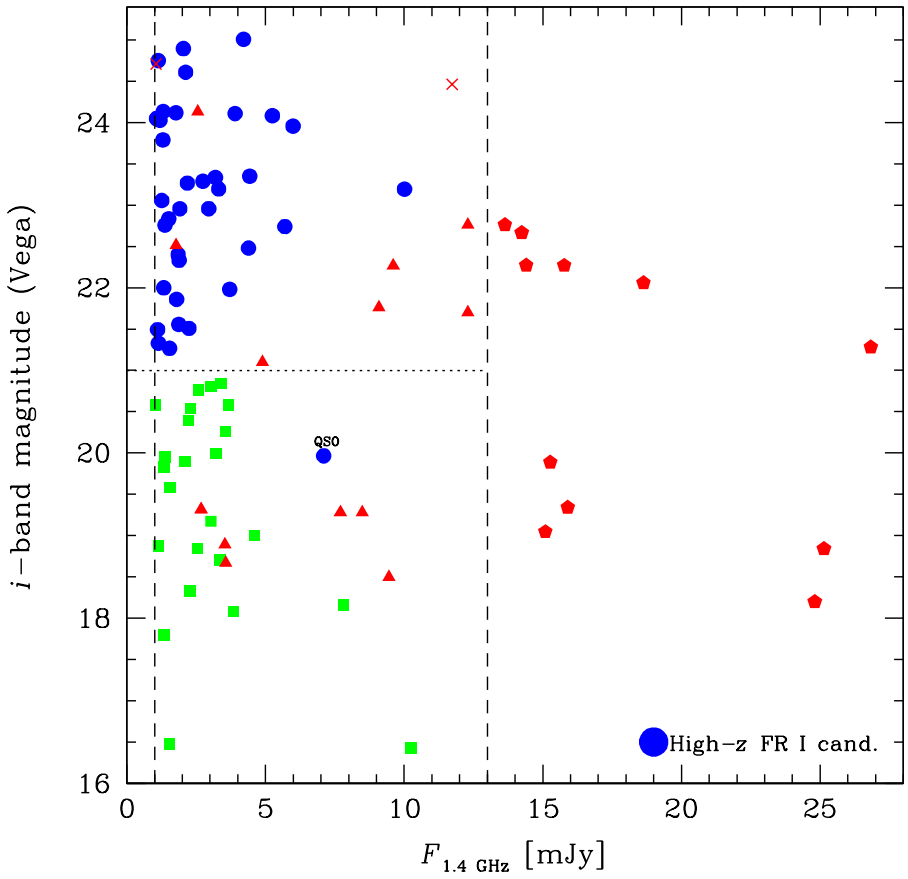

Fig. 3.— Optical i-band magnitude plotted against the radio flux at 1.4 GHz. Only the sources for which a host galaxy is clearly detected are plotted. The two vertical dashed lines are the radio flux limits for the selection process at step 1. The horizontal line represents our lower limit for the optical selection (step 3). Circles are the FR I candidates, triangles are rejected because of their FR II radio morphology, pentagons are rejected by radio flux, squares are rejected by host galaxy magnitude and crosses are u-band dropouts. Note that the QSO is not rejected despite its bright optical magnitude (see text).

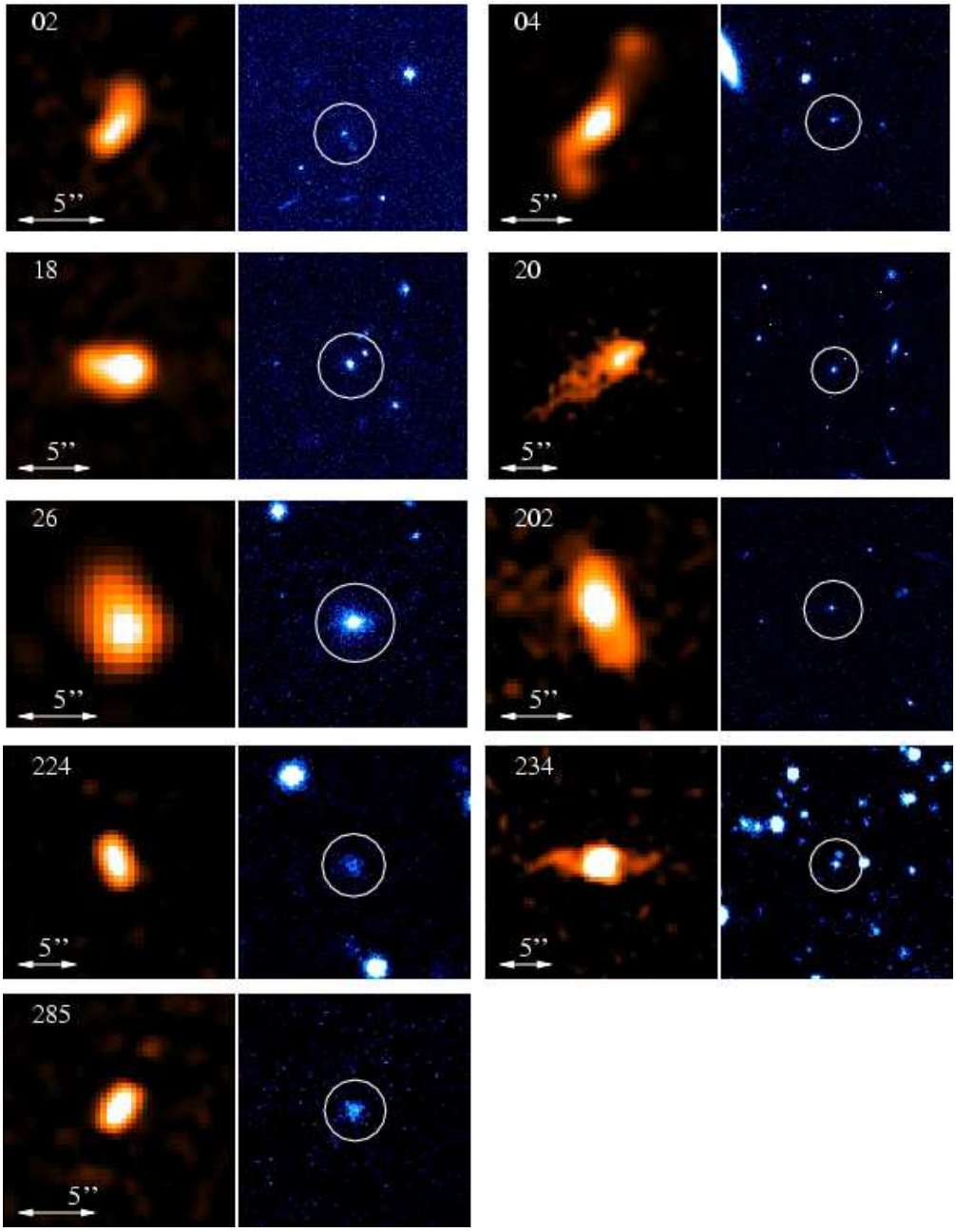

Fig. 4.— FR I candidates with extended 1.4 GHz radio morphology. In these images, 5” corresponds to a linear scale of ~ 40 kpc at $z = 1.5$. For each object, the image in the left panel are from VLA-COSMOS survey, while in the right panel we show the HST-COSMOS ACS images (F814W), except for 234 and 285 where the Subaru i-band image is shown.

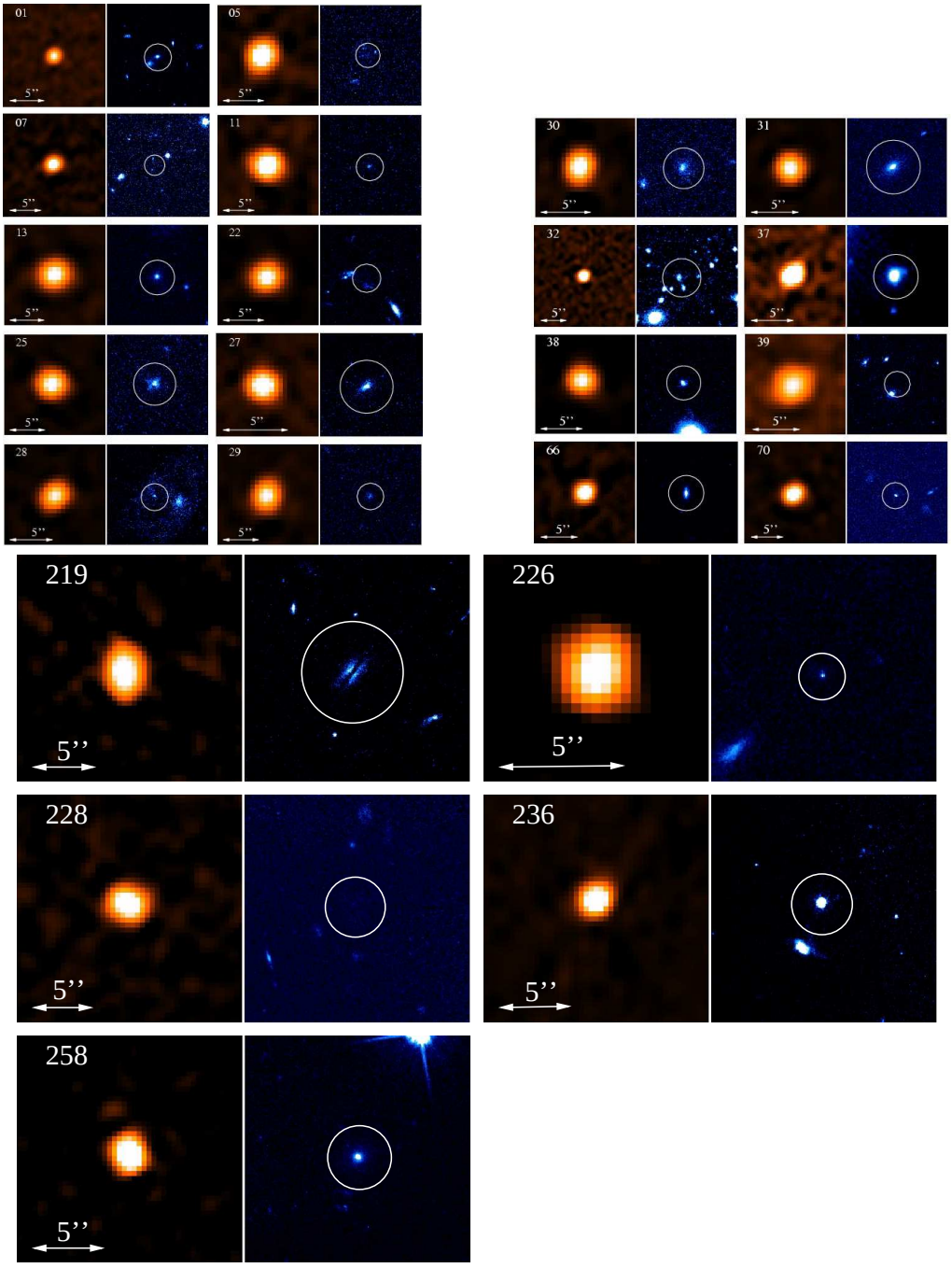

Fig. 5.— FR I candidates with compact (only slightly resolved at the resolution provided by the VLA images) radio morphology. For each object, the image in the left panel is from VLA-COSMOS survey, while in the right panel we show the HST-COSMOS ACS images (F814W), except for objects 32 and 37 where the Subaru i-band image is shown, since the HST image is not available for those two objects.

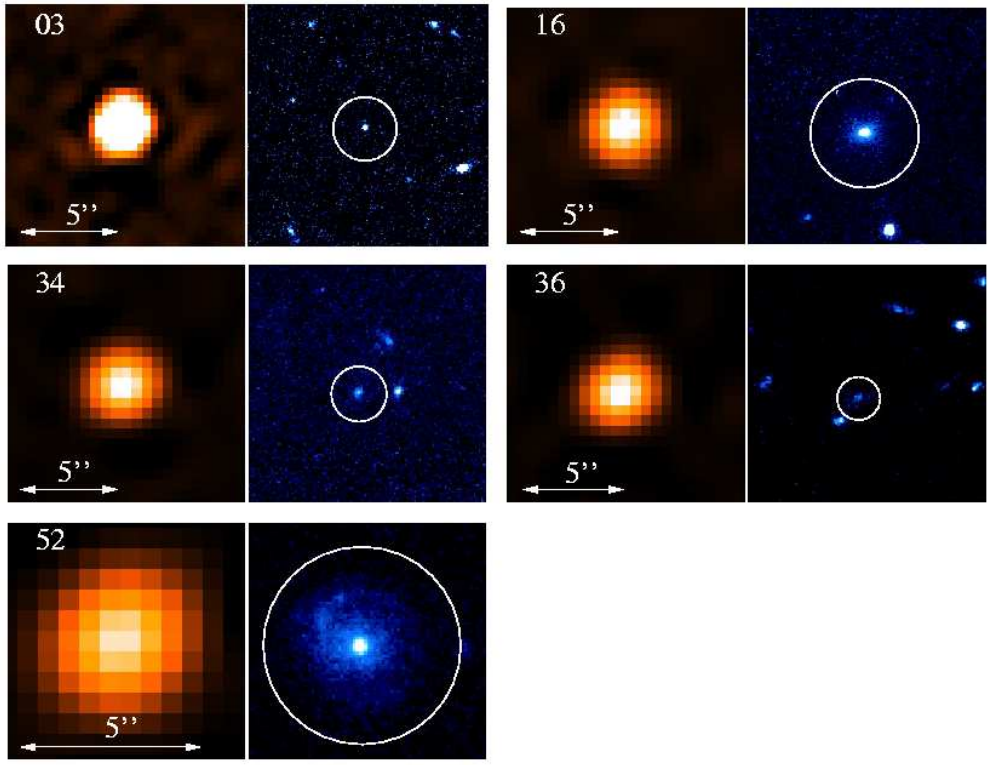

Fig. 6.— FR I candidates with unresolved radio morphology (the FWHM of the source is consistent with the beam width of the VLA image). For each object, the image in the left panel is from VLA-COSMOS survey. In the right panel we show the HST-COSMOS ACS images (F814W)

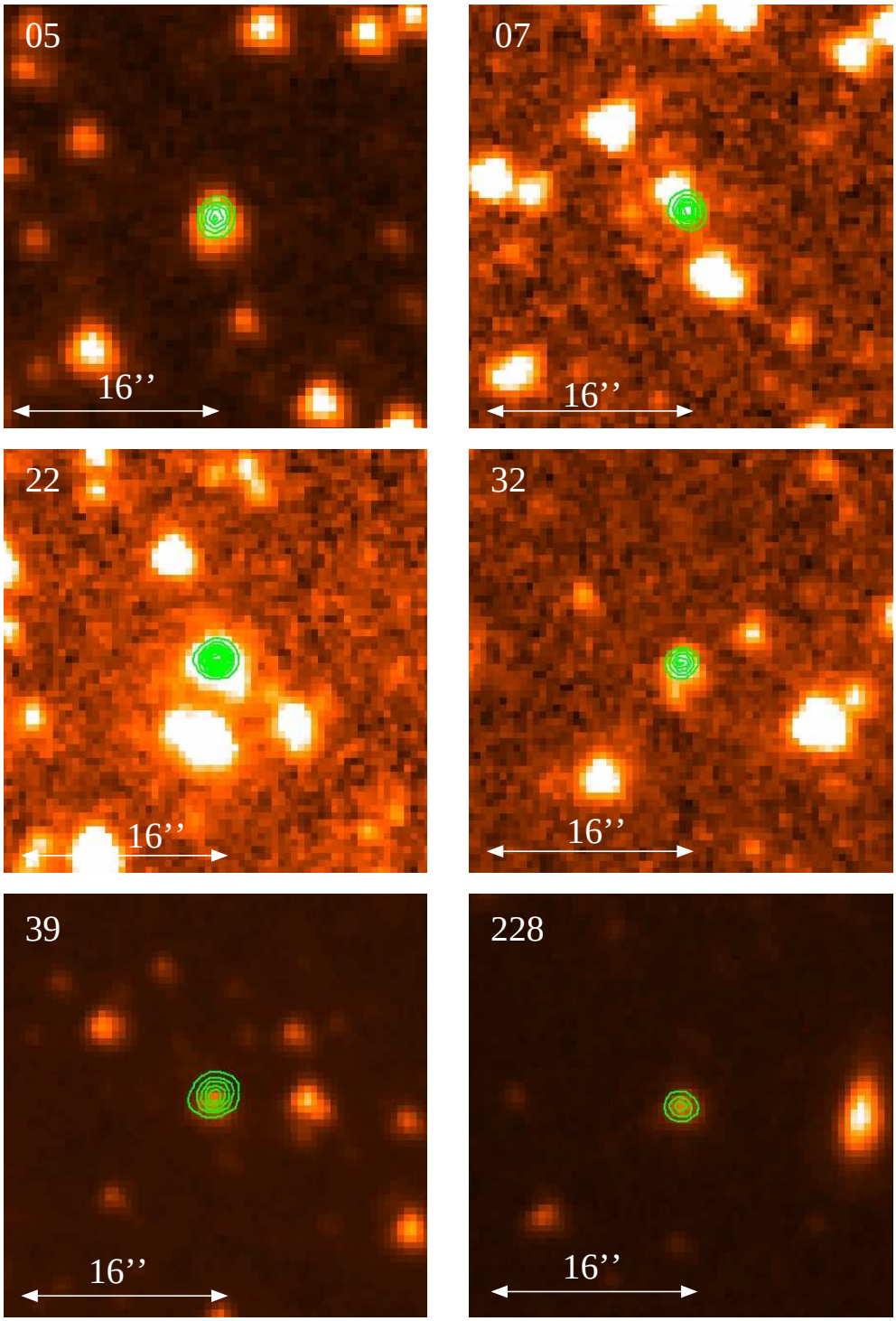

Fig. 7.— Objects identified using *Spitzer* IR images. The radio contours are overplotted onto the 3.6μ image to show the location of the source.

Table 1—Continued

ID	K_s Mag	V Mag	I Mag	$S_{20\ \mathrm{cm}}$ (mJy)	z_{phot}	Radio Morphology	Optical Morphology
(1)	(2)	(3)	(4)	(5)	(6)	(7)	(8)
34	19.105	25.152	24.082	5.25	2.04	Unresolved	Compact
36	18.606	24.782	23.335	3.19	1.42	Unresolved	Complex
37	18.176	22.388	21.556	1.87	1.26	Compact	Smooth
38	19.489	24.603	23.193	10.01	1.15	Compact	Complex
39	18.405	25.268	22.759	1.37	1.36	Compact	–
52	17.928	23.132	21.266	1.54	0.84	Unresolved	Complex
66	18.149	23.637	21.493	1.11	0.80	Compact	Smooth
70	19.521	24.766	24.109	3.90	2.75	Compact	–
202	19.706	26.376	24.049	1.08	1.24	Extended	Compact
219	18.256	24.517	22.402	1.85	1.20	Compact	Complex
224	18.636	25.414	23.196	3.31	1.40	Extended	Compact
226	19.879	25.225	24.027	1.19	2.04	Compact	Compact
228	19.379	27.163	24.894	2.04	1.45	Compact	–
234	18.724	25.399	23.350	4.43	1.42	Extended	Complex
236	17.461	20.594	19.965	7.10	1.23	Compact	QSO
258	17.860	23.190	21.508	2.24	1.07	Compact	Compact
285	19.018	24.022	22.958	2.95	1.24	Extended	Complex

Note. — (1) Object ID; (2) K_s-band apparent magnitude in the Vega system; (3) V-band apparent magnitude (Vega). The magnitude for the objects identified in the IR only are that of the closest optical counterpart; (4) I-band apparent magnitude (Vega). The magnitude for the objects identified in the IR only are that of the closest optical counterpart (Capak et al. 2007); (5) Integrated radio flux at 20 cm (mJy) from the FIRST survey; (6) Photometric redshift $z_{\rm phot}$, calculated by Mobasher et al. (2007); (7) Qualitative characterization of radio morphology, based on VLA-COSMOS image. This classification reflects whether the corresponding image of this target is located in Figs. 4, 5, 6 ; (8) Qualitative characterization of the morphology of the optical counterpart to the radio source, based on inspection of the ACS I-band image. The optical morphology classification for the host galaxies detected only in the IR is omitted.

5. Results and discussion

5.1. The $K - z$ relation

Radio galaxies are known to obey the so-called $K - z$ relation (Lilly & Longair 1982), a correlation between the infrared K-band magnitude and redshift, up to at least $z \sim 4$ (e.g. Jarvis et al. 2003). The origin of the $K - z$ relation is still unclear, and it is possible that it is just the result of selection effect (Lacy 2004). Our selection criteria make use of the optical-IR properties of the hosts of known powerful radio galaxies, which obey the $K - z$ relation. However, while it is important to reject "bright" optical hosts in order to eliminate nearby galaxies from the sample, our selection criteria do not impose any lower limit to the K-band flux of the hosts. In other words, objects that lie significantly above or below the $K - z$ relation are included in our final sample, if they exist at all.

In Fig. 8 we plot the K_s-band magnitude of our FR I candidates' optical counterparts vs. their photometric redshift $z_{\rm phot}$, as derived from the COSMOS photometric catalog by Mobasher et al. (2007). The FR I candidates are plotted as filled circles. The objects that have $m_I < 21$, are plotted as squares. The candidates morphologically identified as FR IIs are not plotted, as in this paper we only focus on FR Is.

In addition to our candidates, we also plot in Fig 8 (as empty circles) the galaxies from the 3CRR, 6C, and 7C catalogs of radio sources (Willott et al. 2003). Whereas for our FR I candidates we plot K_s-band magnitude vs. *photometric* redshift, for the Willott et al. (2003) data we plot K-band magnitude vs. *spectroscopic* redshift. The brightness difference between K- and K_s- bands is typically less than a tenth of a magnitude, therefore the minor differences that arise from comparing photometric measurements in these two bands are not a concern.

As expected from our selection criteria, the objects plotted as squares are relatively

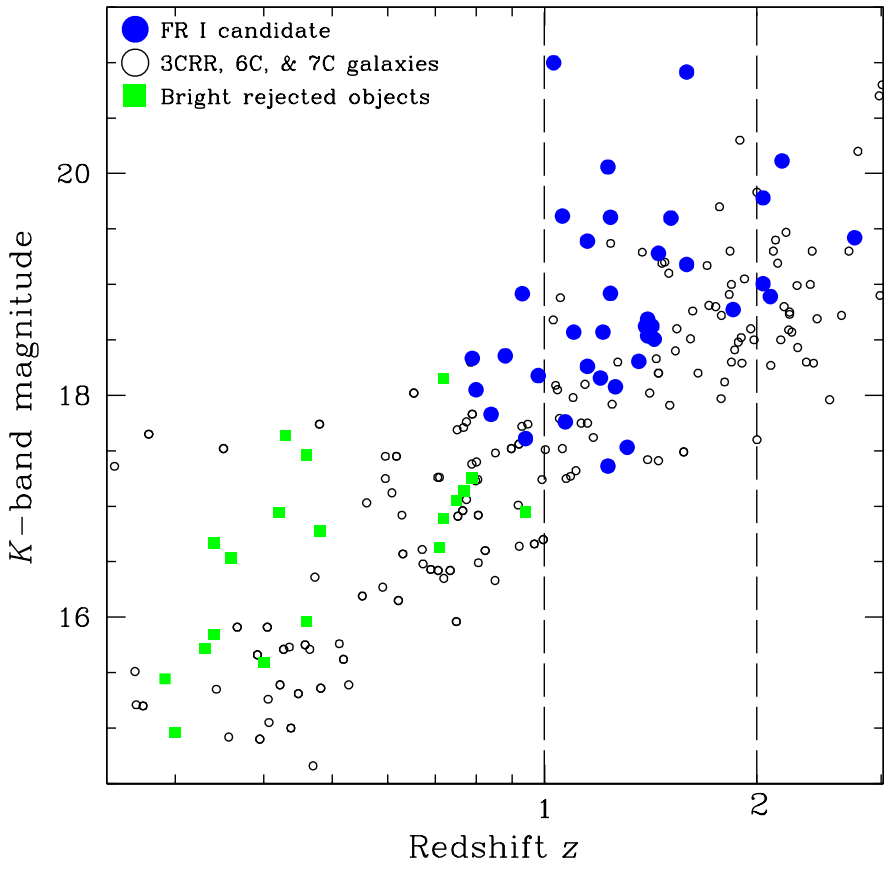

Fig. 8.— The K-z relation for radio galaxies. 3C, 6C and 7C sources from Willott et al. (2003) are plotted as open circles. Our FR I candidates are filled circles. Objects rejected by host galaxy optical magnitude are plotted as squares.

nearby galaxies. With only a few exceptions, the FR I candidates approximately reside in the right redshift bin and lie on the $K - z$ relation or slightly above it. One outlier (object 70) is at $z_{\rm phot} = 2.75$, which is unexpected because our selection procedure should exclude galaxies at $z \gtrsim 2.5$ (u-band dropouts), hence the photometric redshift for object 70 may be incorrect. A few objects are $K \sim 2$mag fainter than the average of the galaxies of Willott et al. (2003). These might be objects for which the photometric redshift is incorrect. Alternatively, they might be a population of radio galaxies associated with fainter hosts. A few objects with $K \sim 2$mag fainter than the bulk of the radio galaxy population is in fact observed at low redshifts as well.

In the following section we describe the FR I candidates, focusing on their radio morphology, properties of the host and Mpc-scale environment.

5.2. Radio Morphology

Here we examine the structure of the 1.4 GHz emission for those 37 FR I candidates appearing as filled circles in Fig. 8. Even at the resolution of the VLA-COSMOS survey most of our targets appear as compact radio sources. Nine of them show a discernible radio morphology on scales larger than $\sim 5''$, which corresponds to a physical scale of ~ 40 kpc at $z = 1.5$.

We show the 1.4 GHz COSMOS VLA images of these nine sources in Fig 4 (left panels), alongside the i-band *HST*/ACS imaging of their optical counterparts (right panels). The optical counterparts are marked with white circles in the HST images.

Even among these sources with extended radio morphology, only two of them (objects 04 and 234) have the radio morphology of "bona fide" FR Is, in which the surface brightness peaks near the center of the source, and extended jets are visible. In objects 02, 18 and

202 the jet seems to be one-sided and curved, similarly to many "asymmetric" nearby FR I galaxies, as they would appear in shallow observations and with poor spatial resolution (e.g. 3C 66B, 3C 129 van Breugel & Jagers 1982). Objects 18 and 26 have a radio morphology similar to the compact radio sources named "core-jet" (Conway et al. 1994), in which the visible jet component is almost as bright as the radio core. The absence of the counter-jet in these objects might be due to relativistic beaming effects, if the jet axis is close to the line-of-sight to the observer.

Object 20 has a very peculiar morphology. It shows a bright compact component, with a possible short jet pointing approximately to the N-W. The "small-scale" morphology is embedded in a larger scale structure with lower surface brightness, similar to an elongate "lobe". Its peculiar morphology might also look like a lobe of an FR II, in which the brightest region is the so-called "hot-spot", usually interpreted as the location where the relativistic jet impacts the ISM/ICM. Therefore, we checked whether a "counter-lobe" was present at some distance along the NW-SE direction. No radio source that could be reasonably interpreted as the "counter-lobe" is found, even allowing for the counter-jet to be slightly bent. That, and the clear correspondence of the brightest radio component with a galaxy in the HST image, lead us to rule out that this object could be the hotspot of an FR II.

All other 28 sources are slightly resolved (Fig 5) or unresolved (Fig 6). However, these observations are at 1.4 GHz, which at $z = 1.5$ corresponds to rest-frame 3.5 GHz. The emission at that frequency is dominated by the central region of the radio source, where young, high energy electrons reside and emit synchrotron radiation up to high radio frequencies, with flat ($\alpha \lesssim 0.5$, where α is defined as $S_\nu \propto \nu^{-\alpha}$) radio spectra. Extended radio components such as jets and lobes have steeper spectra, thus the emission drops as frequency increases. It may therefore be that we simply do not detect extended, low surface

brightness radio jets and lobes for the majority of our candidates given the high rest-frame radio frequency of the observations and the intrinsic faintness of the extended regions.

Note also that the size of the radio sources with "FR I-like" radio structures is smaller than the typical size scales for FR Is at low redshift. Whereas the largest structure we observe among our 37 candidates is of order 100 kpc from end to end (candidate 04, Fig. 4), FR Is in the nearby universe are known to exhibit larger morphologies, up to a few hundreds of kpc, and in a few cases even Mpc, (e.g. B2 1108+27, NGC 6251 Perley et al. 1984).

Although it is likely that the non-detection of large-scale structures is a result of the high frequency at which the COSMOS observations are performed, it is also possible that our high-z FR I candidates are intrinsically small. In fact, even the higher power FR IIs in this redshift range appear smaller than their lower redshift counterparts. From the work by e.g. Kapahi (1985); Gopal-Krishna & Wiita (1987); Kapahi (1989) it is known that the projected linear distance between the hotspots appears to scale roughly as $(1 + z)^{\sigma}$, where σ is between 1 and 2.

Interestingly, Drake et al. (2004) have found a population of infrared-bright radio sources that morphologically resemble the so-called compact steep spectrum (CSS) sources. CSSs are believed to be young radio source that will eventually evolve in the large, powerful FR II radio galaxies. The sources of Drake et al. (2004) are at least 1 dex less powerful than normal CSSs, and the derived expansion velocities of the radio sources are also significantly smaller. From the analysis of their overall properties, these authors claim that those mini-radio sources will not evolve into either FR IIs or FR Is, but will instead lose their radio-loudness and will become radio quiet FIR-luminous AGNs. Should our candidates be intrinsically small, they might "fill the gap" between the powerful CSS sources and the radio-faint sources of Drake et al. (2004), from the point of view of their radio properties. It is thus possible that most of our targets are just the progenitors of the FR Is we observe

in the local universe.

Summarizing, unlike local FR Is, the vast majority of our candidates show very little extended morphology in the radio band. Clearly, it is mandatory to investigate whether that is only due to the high radio frequency at which the observations were made, to the faintness of the extended jets and plumes, or to the fact that our objects may be intrinsically small and possibly young radio sources. The use of the EVLA and ALMA will be necessary in order to achieve sufficient signal to noise ratio and spatial resolution to study these faint and distant objects in more details in the radio band.

5.3. Host Galaxies and environment

We now discuss the optical sources we have identified as host galaxies for the candidate FR I. Optical images for each of these galaxies are shown in Figs. 4, 5 and 6. The photometric properties of the hosts, as derived by Capak et al. (2007), are reported in in Table 1.

Even if the images are single orbit HST pointings, we can attempt to classify the hosts into four different classes, based on their appearance: (1) smooth ellipticals, (2) complex, (3) compact and (4) unresolved. A more detailed study will be performed when deeper images are obtained. Class 1 are objects of apparent elliptical shape, with very little or no disturbed morphology; class 2 are objects that appear to be interacting with close companions and/or show irregular morphologies; class 3 are barely resolved galaxies, too small to discern their properties; class 4 includes the object that we classify as a possible QSO, i.e. a point source is the only obviously detected feature (object 236, Fig. 9)

From visual inspection of the images of the 31 sources with optical counterparts, 6 of our objects appear as smooth ellipticals, 10 are complex, 14 are compact, and 1 is

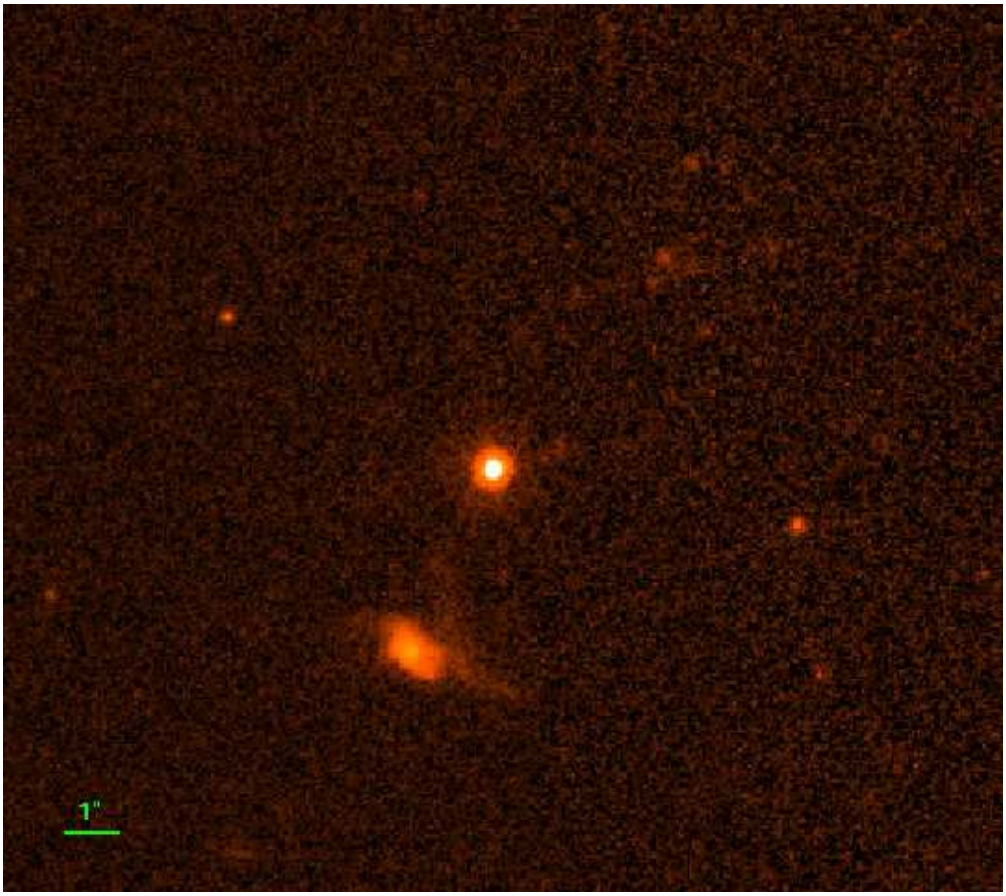

Fig. 9.— HST/ACS F814W image of target 236. The optical counterpart of this object appears as "stellar-like". This might be an example of a low power radio galaxy associated with a QSO.

unresolved (stellar-like). The resolution of the images of the 6 host galaxies that are only detected in the IR does not allow us to derive any morphological classification. It is worth noting the high fraction of objects with complex optical morphologies among our FR I candidates. This appears to be at odds with low redshift FR Is, the large majority of which are hosted by undisturbed ellipticals or cD galaxies (Zirbel 1996). However, the larger fraction of complex morphologies in our sample may simply reflect the different stage of evolution of the host, that might still be in a very active merging phase at $1 < z < 2$.

Not much can be said about the compact galaxies. Because of the short exposure times of the HST data, we might just be seeing the core of the galaxies, while we are missing the external regions of lower surface brightness. Alternatively, these might be intrinsically smaller objects, which would contrast with local FR I hosts that appear to be invariably associated with giant ellipticals.

The presence of one stellar-like optical counterpart is also intriguing. We interpret this object as a compact nucleus (possibly the AGN) outshining the host galaxy. This corresponds to the morphology observed in QSOs, but scaled down in luminosity by a few orders of magnitude. However, it has been established that at low redshifts no FR Is belonging to the 3CR (Spinrad et al. 1985) or B2 (Fanti et al. 1978) samples are associated with host galaxies of this kind. Most importantly, from the point of view of the physics of their active nucleus, none of them appear to show broad lines in the optical spectrum[2]. Recently, Zamfir et al. (2008) have found no FR I-QSO in a large sample of SDSS-FIRST/NVSS quasars, reinforcing the idea that FR I-QSOs are extremely rare in the local universe.

[2]This is true with the only exception of the peculiar galaxy 3C 120, an object with FR I radio morphology associated with an S0 host showing a spiral-like structure. However, 3C 120 is formally not part of the 3CR catalog of Spinrad et al. (1985).

Clearly, this "nucleated" galaxy need further investigation aimed at determining its nature as a quasar through the detection of broad permitted lines in its rest-frame optical spectrum. However, even if the unresolved object was spectroscopically confirmed as a QSOs, the fraction of FR I quasars in our sample (1/37) would be significantly lower than the fraction of FR II quasars in the same range of redshift, which is around 40% (e.g. Willott et al. 2000). A possible scenario is that the smaller fraction of FR I-QSO as compared to the fraction of FR II-QSO simply results from the dependence of such fraction on luminosity (Willott et al. 2000). This may reflect a reduction of the opening angle of the "obscuring torus" as luminosity decreases (the so called "receding-torus" model). Alternatively, most high-z FR Is may intrinsically lack significant broad emission line region and thermal disk emission as is for the FR Is in low-z samples (e.g. Chiaberge et al. 1999). These issues can be explored with deep imaging to determine the nature of the hosts using HST and with spectroscopy using an 8m-class telescope to determine the presence or absence of any strong broad emission lines.

Although our sample cannot be considered statistically complete, the selection criteria are not biased against the presence of QSOs. Instead, the selection based on the radio flux at 1.4MHz is somewhat biased in favor of core-dominated, relativistically beamed objects, and none of the objects that were rejected because their optical i-band magnitude exceeds our selection limit were point sources. The existence of a large number of FR I-QSOs at intermediate-to-high redshifts has been noted by Heywood et al. (2007). This would imply a strong evolution in the physical properties of radio galaxies with FR I radio morphology, since FR I-QSOs are known to essentially absent at low redshifts. However, besides the different selection criteria, the objects of Heywood et al. (2007) are mostly high power sources, while here we focus on radio galaxies of the same power as low-z FR Is. It is thus possible that at high-z, the FR I break shifts towards higher radio powers.

An in-depth analysis of the properties of the objects in our sample and the implications for the AGN unification scheme will be the subject of future work. However, the limited morphological information we have at this stage seems to show that FR I-QSO represent a tiny fraction of the low-power FR I radio galaxies population at $1 < z < 2$.

5.4. FR I candidates as tracers of high-z galaxy clusters?

One of the motivations for our high-z FR I radio galaxy search is to locate high-z clusters of galaxies. In the local universe, $\sim 70\%$ of the entire population of FR Is is associated with cD-like galaxies (Zirbel 1996), and almost all low-z FR Is reside in clusters of various richness (Zirbel 1997). Only ~ 15 clusters are known to exist between $1 < z < 2$, thus a large sample of FR Is may easily double the number of clusters in that redshift range, assuming that the environment of FR Is does not significantly change with redshift. Although we defer a systematic search for clusters to a forthcoming paper, in this section we qualitatively explore the Mpc environments of our candidate FR I, in order to probe the possibility that their host galaxies reside in clusters, similarly to their low z counterparts.

In order to look for cluster candidates, we followed two different methods. Firstly, we searched the COSMOS catalog for the photometric z of objects that are located inside a region of projected radius 1 Mpc from the FR I candidate. Only in the case of object 02 we find qualitative evidence for an over-density of galaxies around the redshift of our FR I candidate, which we interpret as a possible presence of a group or a cluster. In Fig. 10 we show the photometric redshifts distribution of optical sources within $100''$ (corresponding to a projected radius of 855kpc at $z = 1.6$) of candidate 02. The vertical dashed line marks the photometric redshift of the FR I candidate. A peak in the redshift distribution corresponding to the redshift of our source is evident. However, the low detection rate obtained with the above method is not surprising. Our FR I candidates are quite possibly

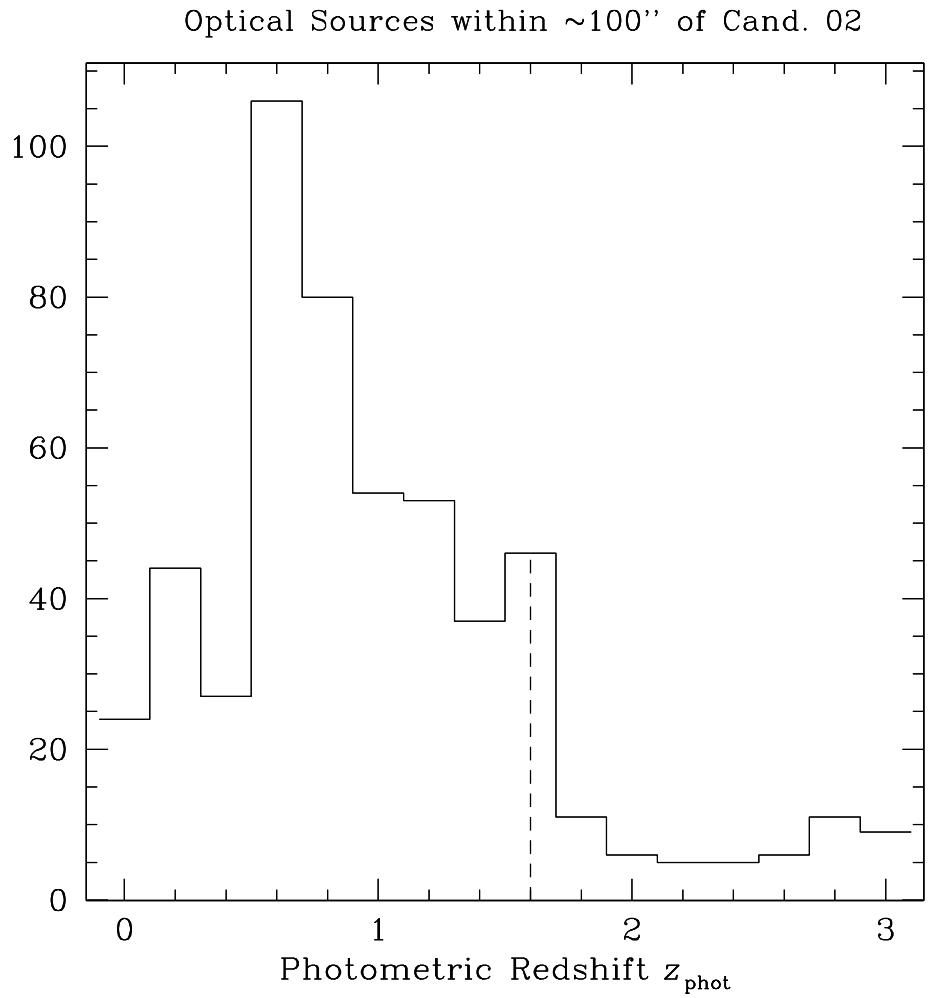

Fig. 10.— Photometric redshifts distribution of optical sources in the COSMOS catalog within $100''$ of candidate 02. The vertical dashed line marks the photometric redshift of the candidate FR I. A peak in the redshift distribution corresponding to the redshift of our source is evident, and may be interpreted as the presence of an overdensity of galaxies at the redshift of the FR I candidate.

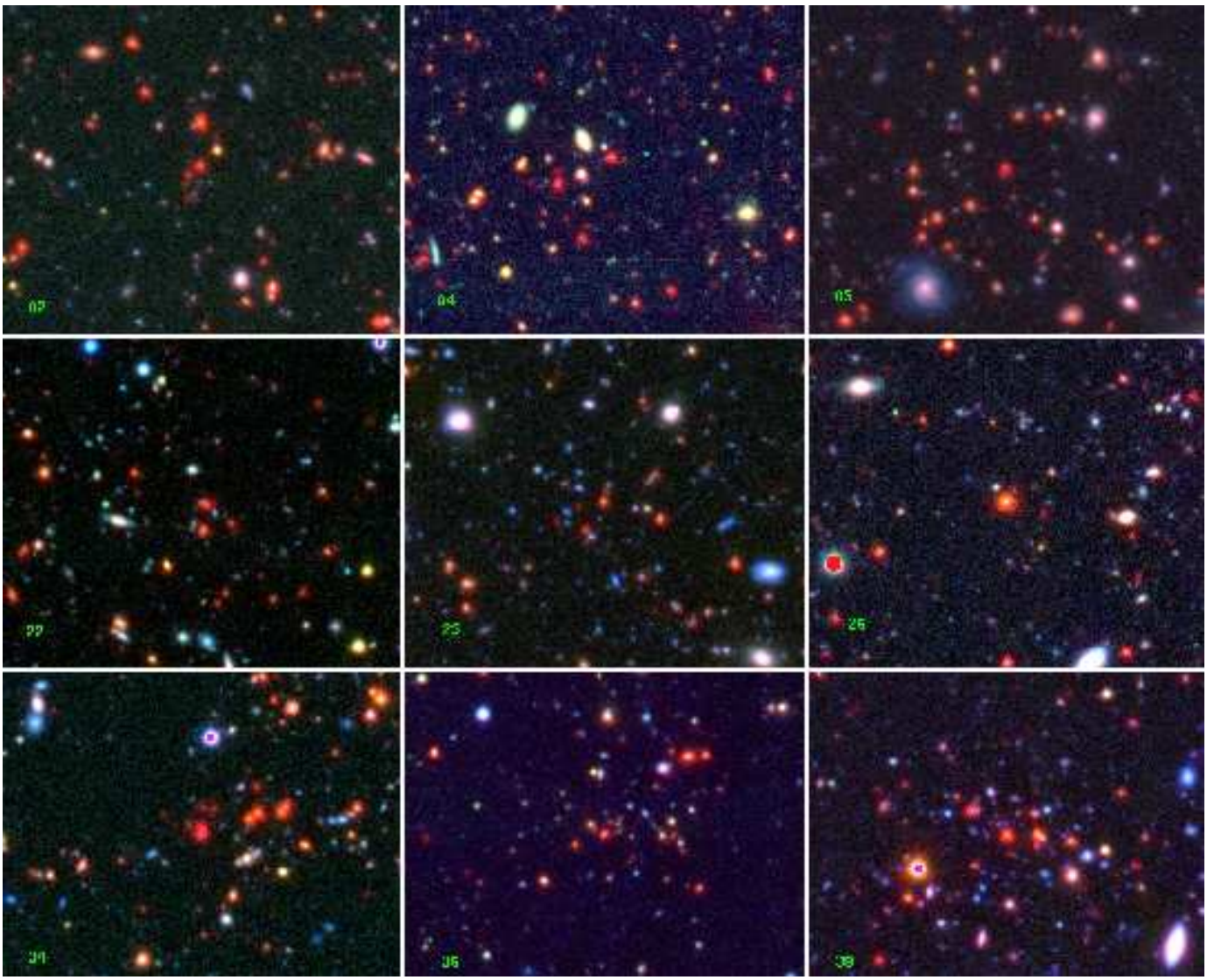

Fig. 11.— RGB images of nine cluster candidates found around our high-z FR I candidates. The "color" images are obtained using *Spitzer* data at 3.6μm for the R channel, z-band for the G channel, and V-band for the B channel. The projected scale of each image is $\sim 110'' \times 90''$

among the brightest cluster members, while an L^* galaxy at $z \sim 1.5$ is expected to have $m_I \sim 24$. Thus, the COSMOS optical images are in fact not deep enough to detect a significant number of cluster galaxies at redshifts $z > 1$. And even when they are detected in the images, their photometric z can be highly uncertain because of the large errors on photometry of such faint objects.

Another, more effective, method we explored to find cluster candidates using the data from COSMOS, is to look for extremely red objects around our FR I candidates. Although there is still some level of degeneracy between objects that are intrinsically red and redshifted objects, this method seems to lead to more promising results, even at the qualitative level presented here. In Fig. 11 we show nine cluster candidates found with the latter method. We produced RGB "color" images using *Spitzer Space Telescope* data at 3.6μm for the R channel, z-band for the G channel, and V-band for the B channel. We are setting up observational programs to measure the redshift of the brightest cluster members and we will systematically study cluster candidates in a forthcoming paper.

In order to achieve more detailed information about the morphology of the host galaxies, their possible interactions with immediate neighbors, and the properties of the cluster environment, deep high-resolution optical and near-IR images and possibly slitless spectroscopy should be obtained as soon as the WFC3 is installed on HST. Only the future generation of high-sensitivity X-ray telescopes (e.g. IXO) will allow us to study in detail the properties of any hot virialized gas in the cluster environment of our sources. However, in a forthcoming paper we will study the *Chandra*/COSMOS data to try and detect such a hot gas using stacking techniques.

6. Summary & Conclusions

We have outlined our search for FR I radio galaxy candidates in the COSMOS field at redshift $1 < z < 2$. Previously, no low power FR I radio galaxies were known in this redshift bin, besides one (or possibly two) candidate in the HDF North (Snellen & Best 2001). Flux limited samples are not suitable for finding low-power radio galaxies at high-z, because of the tight redshift-luminosity correlation. Therefore, we used a 4-steps multi-wavelength selection process, starting from radio flux, and using radio morphologies and optical magnitudes to further constrain the sample selection. At the end of the selection process we are left with a sample of 37 objects.

The photometric redshift of the bulk of our FR I candidates are in the expected range $1 < z_{\rm phot} < 2$. The redshifts must be confirmed with spectroscopic observations possibly using at least an 8m-class telescope, future larger instruments or space-based observations to take advantage of the lower background. In most cases, the radio images show objects with compact morphologies. These might be intrinsically young sources, that will eventually evolve into the giant FR I radio galaxies observed at low redshifts. Alternatively, the extended emission is not detected because of the rest-frame high frequency at which the observations were taken. Further investigation is needed to address this issue. We plan on obtaining low-frequency radio observations to detect any extended radio emission from "older" electrons, combined with deep, high resolution data at a higher wavelength (~ 8 GHz) to derive the spectral index of the source and to study the morphology.

The short one-orbit i-band HST observations are not suitable for a detailed morphological study of the host galaxies. However, the data show variegated morphologies, ranging from smooth ellipticals to complex interacting systems. A few of them appear to be compact and one is stellar-like. This object might belong to a population of FR I-QSOs that is basically not present in the local universe. However, the fraction of low-power

FR I-QSOs in our sample appears to be significantly lower than the overall fraction of FR II-QSOs in the same redshift bin. Optical-IR spectroscopy of the sources is needed to assess the nature of this candidate QSO.

Although the images from the COSMOS survey are not suitable to detect a large fraction of cluster galaxies at $z > 1$, the environment of some of our FR I candidates shows evidence for the presence of a cluster. This is apparent when the IR images from the *Spitzer* space telescope are used in combination with the optical ground based data, resulting in a significant number of red objects surrounding the host galaxies of our FR I candidates.

The search for high-z FR I candidates we presented in this paper constitutes a pilot study for objects to observed with high-resolution and high-sensitivity future instruments. The EVLA and ALMA will provide us with crucial information on the radio morphology of our sources, they will help us to understand whether or not the objects we discovered are intrinsically small, and if they are "progenitors" of the local FR I population. When WFC3 is installed on the HST, it will be possible to study in greater details the properties of the host galaxies and the cluster environment in the optical and IR, with important bearings for our knowledge of the origin of the most massive galaxies and galaxy clusters. Clearly, these studies will be complemented and further expanded when JWST will be available, as well as when future generation high-sensitivity X-ray satellites will be launched.

We are indebted with the referee for her/his comments that greatly improved the paper. We are grateful to Piero Rosati, Stefi Baum and Meg Urry for helpful discussions. GRT acknowledges support from HST-GO-10882.01-A. We acknowledge the effort of the entire COSMOS team without which this work would not have been possible. More information on COSMOS is available at `http://cosmos.astro.caltech.edu`. The *Very Large Array* is a facility of the National Radio Astronomy Observatory, operated by Associated Universities, Inc., under cooperative agreement with the National Science Foundation. This research

has made use of the NASA/ IPAC Infrared Science Archive, which is operated by the Jet Propulsion Laboratory, California Institute of Technology, under contract with the National Aeronautics and Space Administration.

REFERENCES

Baum, S. A., Zirbel, E. L., & O'Dea, C. P. 1995, ApJ, 451, 88

Becker, R. H., White, R. L., & Helfand, D. J. 1995, ApJ, 450, 559

Blandford, R. D., Netzer, H., Woltjer, L., Courvoisier, T. J.-L., & Mayor, M. 1990, Active Galactic Nuclei (Saas-Fee Advanced Course 20. Lecture Notes 1990. Swiss Society for Astrophysics and Astronomy, XII, 280 pp. 97 figs.. Springer-Verlag Berlin Heidelberg New York)

Blanton, E. L., Gregg, M. D., Helfand, D. J., Becker, R. H., & White, R. L. 2000, ApJ, 531, 118

Capak, P., et al. 2007, ApJS, 172, 99

Chiaberge, M., Capetti, A., & Celotti, A. 1999, A&A, 349, 77

Conway, J. E., Myers, S. T., Pearson, T. J., Readhead, A. C. S., Unwin, S. C., & Xu, W. 1994, ApJ, 425, 568

Donzelli, C. J., Chiaberge, M., Macchetto, F. D., Madrid, J. P., Capetti, A., & Marchesini, D. 2007, ApJ, 667, 780

Drake, C. L., Bicknell, G. V., McGregor, P. J., & Dopita, M. A. 2004, AJ, 128, 969

Eracleous, M., & Halpern, J. P. 1994, ApJS, 90, 1

Fabian, A. C., Sanders, J. S., Crawford, C. S., & Ettori, S. 2003, MNRAS, 341, 729

Fabian, A. C., Sanders, J. S., Taylor, G. B., Allen, S. W., Crawford, C. S., Johnstone, R. M., & Iwasawa, K. 2006, MNRAS, 366, 417

Falcke, H., Körding, E., & Markoff, S. 2004, A&A, 414, 895

Fanaroff, B. L., & Riley, J. M. 1974, MNRAS, 167, 31P

Fanti, R., Gioia, I., Lari, C., & Ulrich, M. H. 1978, A&AS, 34, 341

García-Lorenzo, B., Sánchez, S. F., Mediavilla, E., González-Serrano, J. I., & Christensen, L. 2005, ApJ, 621, 146

Giavalisco, M. 2002, ARA&A, 40, 579

Gopal-Krishna, & Wiita, P. J. 1987, MNRAS, 226, 531

Heywood, I., Blundell, K. M., & Rawlings, S. 2007, MNRAS, 381, 1093

Hopkins, P. F., Somerville, R. S., Hernquist, L., Cox, T. J., Robertson, B., & Li, Y. 2006, ApJ, 652, 864

Jarvis, M. J., Rawlings, S., Eales, S., Blundell, K. M., & Willott, C. J. 2003, in The Mass of Galaxies at Low and High Redshift, ed. R. Bender & A. Renzini, 148–+

Kapahi, V. K. 1985, MNRAS, 214, 19P

—. 1989, AJ, 97, 1

Koekemoer, A. M., et al. 2007, ApJS, 172, 196

Lacy, M. 2004, in Coevolution of Black Holes and Galaxies, ed. L. C. Ho

Ledlow, M. J., & Owen, F. N. 1996, AJ, 112, 9

Lilly, S. J., & Longair, M. S. 1982, MNRAS, 199, 1053

Livio, M. 1999, Phys. Rep., 311, 225

Miley, G., & De Breuck, C. 2008, A&A Rev., 1

Mobasher, B., et al. 2007, ApJS, 172, 117

Owen, F. N. 1996, Extragalactic Radio Sources, 175, 305

Owen, F. N., & Ledlow, M. J. 1994, in Astronomical Society of the Pacific Conference Series, Vol. 54, The Physics of Active Galaxies, ed. G. V. Bicknell, M. A. Dopita, & P. J. Quinn, 319–+

Pentericci, L., McCarthy, P. J., Röttgering, H. J. A., Miley, G. K., van Breugel, W. J. M., & Fosbury, R. 2001, ApJS, 135, 63

Perley, R. A., Bridle, A. H., & Willis, A. G. 1984, ApJS, 54, 291

Rosati, P., Borgani, S., & Norman, C. 2002, ARA&A, 40, 539

Sadler, E. M., et al. 2007, MNRAS, 381, 211

Sanders, D. B., et al. 2007, ApJS, 172, 86

Scarpa, R., & Urry, C. M. 2001, ApJ, 556, 749

Schinnerer, E., et al. 2007, ApJS, 172, 46

Scoville, N., et al. 2007, ApJS, 172, 1

Snellen, I. A. G., & Best, P. N. 2001, MNRAS, 328, 897

Spinrad, H., Marr, J., Aguilar, L., & Djorgovski, S. 1985, PASP, 97, 932

Taniguchi, Y., et al. 2007, ApJS, 172, 9

Ueda, Y., Akiyama, M., Ohta, K., & Miyaji, T. 2003, ApJ, 598, 886

van Breugel, W., & Jagers, W. 1982, A&AS, 49, 529

Willott, C. J., Rawlings, S., Blundell, K. M., & Lacy, M. 2000, MNRAS, 316, 449

Willott, C. J., Rawlings, S., Jarvis, M. J., & Blundell, K. M. 2003, MNRAS, 339, 173

York, D. G., et al. 2000, AJ, 120, 1579

Zamfir, S., Sulentic, J. W., & Marziani, P. 2008, MNRAS, 387, 856

Zirbel, E. L. 1996, ApJ, 473, 713

—. 1997, ApJ, 476, 489

Zirm, A. W., et al. 2005, ApJ, 630, 68